

MOL #37002

**Role of PKC ζ and its adaptor protein p62 in K_v channel
modulation in pulmonary arteries.**

Laura Moreno¹, Giovanna Frazziano¹, Angel Cogolludo, Laura Cobeño, Juan Tamargo,
Francisco Perez-Vizcaino.

Department of Pharmacology, School of Medicine, Universidad Complutense de Madrid,
28040 Madrid, Spain

MOL #37002

Running title: Role of PKC ζ and p62 in K_V channel modulation.

Correspondence to:

Francisco Perez-Vizcaino. Department of Pharmacology. School of Medicine. Universidad Complutense. 28040 Madrid. Spain. Phone: 34-913941477; Fax: 34-913941470. Email:

fperez@med.ucm.es

Number of text pages: 26

Number of tables: 0

Number of figures: 6

Number of references: 37

Number of words in Abstract: 190

Number of words in Introduction: 715

Number of words in Discussion: 1285

Nonstandard abbreviations: aPKC, atypical PKC; Ca_L, voltage-dependent L-type Ca²⁺ channels; DPO-1, ([1S-1 α ,2 α ,5 β]-[5-Methyl-2-(1-methylethyl) cyclohexyl] diphenyl phosphine oxide); K_V, voltage-gated K⁺ channels; PA, pulmonary artery; PASMC, pulmonary artery smooth muscle cells; PH, pulmonary hypertension; PKC ζ , protein kinase C ζ ; PKC ζ -PI, PKC ζ pseudosubstrate inhibitory peptide; TP, thromboxane-endoperoxide receptors; TXA₂, thromboxane A₂; U46619, 9,11-dideoxy-11 α ,9 α -epoxymethano-prostaglandin F_{2 α} .

MOL #37002

Abstract: Voltage-gated potassium (K_V) channels play an essential role in regulating pulmonary artery function and underpin the phenomenon of hypoxic pulmonary vasoconstriction. Pulmonary hypertension is characterised by inappropriate vasoconstriction, vascular remodelling and dysfunctional K_V channels. In the current study we aimed to elucidate the role of PKC ζ and its adaptor protein p62 in the modulation of K_V channels. We report that the thromboxane A_2 analogue U46619 inhibited K_V currents in isolated mice pulmonary artery myocytes and the K_V current carried by human cloned $K_V1.5$ channels expressed in Ltk $^-$ cells. Using PKC $\zeta^{-/-}$ and p62 $^{-/-}$ mice, we demonstrate that these two proteins are involved in the K_V channel inhibition. PKC ζ co-immunoprecipitated with $K_V1.5$ and this interaction was markedly reduced in p62 $^{-/-}$ mice. Pulmonary arteries from PKC $\zeta^{-/-}$ mice also showed a diminished $[Ca^{2+}]_i$ and contractile response while genetic inactivation of p62 $^{-/-}$ resulted in an absent $[Ca^{2+}]_i$ response but preserved contractile response to U46619. These data demonstrate that PKC ζ and its adaptor protein, p62, play a key role in the modulation of K_V channel function in pulmonary arteries. These observations identify PKC ζ and/or p62 as potential therapeutic targets for the treatment of pulmonary hypertension.

MOL #37002

Voltage-gated potassium (K_V) channels play an essential role in regulating vascular smooth muscle function. They make a substantial contribution to whole-cell K^+ conductance and resting membrane potential in pulmonary artery smooth muscle cells (PASMC) and its inhibition causes membrane depolarisation, activation of L-type Ca^{2+} channels (Ca_L), increases in $[Ca^{2+}]_i$ and vasoconstriction (Archer et al., 1998; Yuan et al., 1998b; Barnes and Liu, 1995). These channels are common targets of pulmonary vasoconstrictor stimuli such as hypoxia, thromboxane A_2 (TXA_2) endothelin-1 or angiotensin-II (Archer et al., 1998; Shimoda et al., 2001; Cogolludo et al., 2003; 2006). In addition, decreased expression or function of K_V channels in PASMC has been involved in the pathogenesis of pulmonary arterial hypertension (PH) (Weir et al., 1996, Yuan et al., 1998a; Pozeg et al., 2003). From the variety of K_V channels expressed in PASMC (Platoshyn et al., 2006), special interest has been paid to $K_V1.5$, since decreased expression or activity and mutations of $K_V1.5$ occurs in human (Yuan et al., 1998a; Remillard et al., 2007) and experimental (Archer et al., 1998; Pozeg et al., 2003) idiopathic and hypoxic PH, and *in vivo* gene transfer of $K_V1.5$ reduces PH (Pozeg et al., 2003).

TXA_2 is a prostanoid synthesized by cyclooxygenase with potent vasoconstrictor, mitogenic, and platelet aggregant properties via activation of thromboxane-endoperoxide (TP) receptors (Halushka et al. 1989). The vasoconstrictor effects of TXA_2 are particularly pronounced in the pulmonary vascular bed, where it participates in the control of vessel tone under physiological and pathological situations, including PH. We have previously reported that in intact PAs and freshly isolated PASMCs, TXA_2 , via activation of TP receptors, inhibits K_V channels, leading to membrane depolarization, activation of L-type Ca^{2+} channels, and vasoconstriction. Furthermore, using a protein kinase C ζ (PKC ζ) pseudosubstrate inhibitory

MOL #37002

peptide (PKC ζ -PI) we provided evidence for the role of this kinase as a link between TP receptor activation and K_V channel inhibition (Cogolludo et al., 2003; 2005). PKC ζ (together with PKC $\lambda/1$) belongs to the atypical PKC (aPKC) subclass. Both aPKCs play key roles in different signaling pathways regulating cell growth, survival and differentiation (Moscat and Díaz-Meco, 2002). The aPKCs share with other members of their family a conserved catalytic domain but display a clearly distinct regulatory region since they have been shown to be independent of Ca²⁺, diacylglycerol and phorbol esters, all of which are potent activators of other PKC isoforms. PKC ζ is activated by phosphatidylinositols, arachidonic acid and other lipids (Hirai and Chida, 2003) as well as by a variety of mediators including insulin (Liu et al., 2006), thromboxane A₂ (Cogolludo et al., 2003, 2005; Shizukuda and Buttrick, 2002), angiotensin II (Gayral et al., 2006; Godeny and Sayeski, 2006) or pro-inflammatory cytokines (Frey et al., 2006).

The mechanism underlying the activation of aPKCs responsible for its diverse physiological functions remains unclear but several groups have identified a number of aPKC-interacting proteins, including p62 (also called ZIP1 or sequestosome 1), Par-4, Par-6 and MEK5 (Moscat and Diaz-Meco, 2000). Interestingly, nerve growth factor and catecholamines have been reported to increase the expression of p62, enabling the formation of the PKC ζ -p62-K_V β complex which results in a hyperpolarizing shift in the K_V current activation curve (Gong et al., 1999; Kim et al., 2004; 2005).

The role of PKC on pulmonary vasoconstriction has been widely reported (Ward et al., 2004), however many of these studies have been conducted with PKC modulators of dubious selectivity, thereby, limiting their conclusions. Molecular biology and genetic approaches and

MOL #37002

the currently available isoform-selective PKC inhibitors have made possible the elucidation of the involvement of specific PKC isoforms in cellular processes (such as vascular contractility) (Salamanca and Khalil, 2006). However, recent evidences suggest that some considered isoform-specific PKC inhibitors, such as myristoylated PKC ζ pseudosubstrate peptide, may exert other effects unrelated to inhibition of PKC and, thus, should be used with caution (Krotova et al., 2006).

Therefore, in the present study we aimed to further characterize the signalling pathway modulating K_V currents in PA. Using PKC ζ ^{-/-} and p62^{-/-} mice, we provide evidence for the interaction of PKC ζ with K_V channels which further support the role of this interaction in TXA₂-induced effects. In addition, we hypothesized that the PKC ζ -K_V-L-type Ca²⁺ channels pathway might involve other proteins such as p62. This possibility was tested by analyzing the modulation of K_V channels in wild-type and p62 homozygous null mice.

MATERIAL AND METHODS

All experiments were carried out in accordance with the European Animals Act 1986 (Scientific Procedures) and approved by our institutional review board.

Animals

Lungs from PKC ζ ^{-/-} (mixed C57BL/6 and SV129J background), p62^{-/-} (C57BL/6) and corresponding wild-type mice (six to eight week old, either sex) were generously supplied by

MOL #37002

Drs. Moscat and Diaz-Meco which were generated as described (Leitges et al. 2001; Duran et al. 2004). PA from male Wistar rats (250-300 g) were also used in these experiments.

Tissue Preparation and Cell Isolation

Second-order branches of the PA (internal diameter, ≤ 0.5 mm) isolated from mice were dissected into a nominally calcium-free physiological salt solution (Ca^{2+} -free PSS) of the following composition (in mmol/L): NaCl 130, KCl 5, MgCl_2 1.2, glucose 10, and HEPES 10 (pH 7.3 with NaOH). Endothelium denuded PAs were cut into small segments (2x2 mm), and cells were isolated in Ca^{2+} -free PSS containing (in mg/mL) papain 1, dithiothreitol 0.8, and albumin 0.7. Cells were stored in Ca^{2+} -free PSS (4°C) and used within 8 hours of isolation.

Electrophysiological Studies

Membrane currents were measured using the whole-cell configuration of the patch-clamp technique (Cogolludo et al., 2003) normalized for cell capacitance and expressed in pA pF^{-1} . Membrane potential (E_m) was measured under current-clamp configuration. K_V currents were recorded under essentially Ca^{2+} -free conditions using an external Ca^{2+} -free PSS and a Ca^{2+} -free pipette (internal) solution (see solutions section). Ltk⁻ cells stably expressing $\text{hK}_V1.5$ channels (Valenzuela et al., 1995) were superfused with PSS containing 1 mmol/L CaCl_2 . Currents were evoked following the application of 200 ms depolarizing pulses from -60 mV to test potentials from -60 mV to +40 mV in 10 mV increments. All experiments were performed at room temperature (22 to 24°C).

[Ca²⁺]_i recording.

PA rings were incubated for 80 minutes at room temperature in Krebs solution containing the fluorescent dye Fura-2 acetoximethylester (5×10^{-6} M) and cremophor EL (0.05%) and then mounted in a fluorimeter (CAF 110 model, Jasco, Tokyo). PA rings were alternatively illuminated (128 Hz) with two excitation wavelengths (340 and 380 nm) and the emitted fluorescence was filtered at 505 nm (Pérez-Vizcaíno et al., 1998). The ratio of emitted fluorescence (F340/F380) obtained at the two excitation wavelengths was used as an indicator of [Ca²⁺]_i. Arteries were stimulated with 30 nM and 300 nM U46619, added in a cumulative fashion. In preliminary experiments in wild-type mice, these concentrations produced ~60% and ~80% of the maximal response, respectively. The [Ca²⁺]_i signal in each vessel was calibrated according to the Grynkiewicz equation by sequential addition of ionomycin (15 μM) and EGTA (10 mM) at the end of the experiment.

Co-immunoprecipitation and Western blot analysis.

Mice lungs were rapidly frozen in liquid nitrogen. In some experiments, rat PA were placed in warm Krebs solution and then in the absence or presence of U46619 (1 μM) for 30 s and then rapidly frozen. Frozen tissues were homogenized in a glass potter in 200 μL of a buffer of the following composition (mmol/L): HEPES 10 (pH 8), KCl 10, EDTA 1, EGTA 1, dithiothreitol 1, aprotinin 0.006, leupeptin 0.009, Nα-p-tosyl-L-lysine chloromethyl ketone 0.011, NaF 5, Na₂MoO₄ 10, NaVO₄ 1, phenylmethanesulfonyl fluoride 0.5 and okadaic acid 0.00001. Homogenates were centrifuged at 13,000g for 5 min at 4°C and the supernatant fraction was collected. For immunoprecipitation, sixty μg of protein were incubated for 2

MOL #37002

hours with anti-PKC ζ or anti-K $_v$ 1.5 antibody at 4°C, followed by the addition of protein A/G beads and further incubation overnight. These immune complexes or 20 μ g of the homogenates from mice lungs or rat PA were separated by SDS-PAGE and transferred to a PVDF membrane for western blotting as described (Cogolludo et al., 2003). Membranes were probed for K $_v$ 1.5, PKC ζ and p62-like immunoreactivity.

Solutions and Chemicals

For the single cell electrophysiological studies, the composition of the Ca $^{2+}$ -free bath solution (external Ca $^{2+}$ -free PSS) was as follows (mM): NaCl 130, KCl 5, MgCl $_2$ 1.2, glucose 10, HEPES 10, buffered to pH 7.3 with NaOH. The Ca $^{2+}$ -free pipette (internal) solution contained (mM): KCl 110, MgCl $_2$ 1.2, Na $_2$ ATP 5, HEPES 10, EGTA 10, pH adjusted to 7.3 with KOH. The Krebs solution used for tissue bath experiments comprised (in mM): NaCl 118, KCl 4.75, NaHCO $_3$ 25, MgSO $_4$ 1.2, CaCl $_2$ 2.0, KH $_2$ PO $_4$ 1.2 and glucose 11. This solution was gassed with a 95% O $_2$ -5% CO $_2$ gas mixture at 37° C. U46619 (9, 11-dideoxy-11 α ,9 α -epoxymethano-prostaglandin F $_{2\alpha}$ methyl acetate solution) was obtained from Sigma Chemical Co., DPO-1 ([1S-1 α ,2 α ,5 β]-[5-Methyl-2-(1-methylethyl) cyclohexyl] diphenyl phosphine oxide) from Tocris Cookson, secondary horseradish peroxidase conjugated antibodies and fura-2 AM from Calbiochem, rabbit anti-K $_v$ 1.5 from Alomone, goat anti-PKC ζ from Santa Cruz Biotechnology and guinea-pig anti-p62 from Progen.

Statistical analysis.

Data are expressed as means \pm s.e.mean; n indicates the number of arteries or cells tested. All experiments were conducted in arteries or cells from at least four different animals. Statistical

MOL #37002

analysis was performed using Student's t-test for paired or unpaired observations. Differences were considered statistically significant when p was less than 0.05.

RESULTS

Role of PKC ζ in K_V current inhibition induced by TXA₂

A family of K_V currents (I_{K(V)}) were obtained in mice PASMCM when eliciting depolarizing steps from -60 to +40 mV (Fig. 1A and 1B) from a holding potential of -60 mV. The magnitude of the currents, the threshold voltage for activation and the current-voltage relationship (Fig. 1C and 1D) was similar in PASMCM from wild-type and PKC ζ ^{-/-} mice (e.g. current density at +40 mV was 9.1 ± 1.9 and 8.7 ± 0.8 pA pF⁻¹, respectively). Current inactivation was also similar in both strains (i.e. at 200 ms the current decayed by 11.5 ± 3 and 12.1 ± 3.8%, respectively). Currents were recorded before (control) and after addition of the TXA₂ analogue U46619. U46619 (100 nM) caused a significant inhibition of K_V currents in the whole range of channel activation in PASMCM from wild-type mice (Fig. 1A). The degree of current inactivation at +40 mV was increased by U46619 (i.e. at 200 ms the current decayed by 25.6 ± 4.8%, $p < 0.05$). In addition, U46619 induced membrane depolarization in wild-type PASMCM (Fig. 1E). However, U46619 had no effect on either K_V currents or membrane potentials in PASMCM from PKC ζ ^{-/-} mice (Figs. 1B, D, F).

Role of PKC ζ in [Ca²⁺]_i increase and contraction induced by TXA₂

MOL #37002

Changes in $[Ca^{2+}]_i$ and contraction induced by U46619 were simultaneously analyzed in fura-2 loaded PA from wild-type and from $PKC\zeta^{-/-}$ mice. Basal levels of $[Ca^{2+}]_i$ in $PKC\zeta^{-/-}$ (203 ± 40 nM, $n=6$) were not significantly different from those in wild-type mice (160 ± 40 nM, $n=6$). Stimulation of endothelium-denuded PA rings with 30 and 300 nM U46619 induced a sustained elevation in $[Ca^{2+}]_i$ and a contractile response in PA from wild-type and $PKC\zeta^{-/-}$ animals (Fig. 2A and 2B). However, the increase in $[Ca^{2+}]_i$ (Fig. 2C) and the contractile response (Fig. 2D) was significantly reduced in $PKC\zeta^{-/-}$ mice as compared to wild-type mice.

Role of p62 in K_V current inhibition, $[Ca^{2+}]_i$ increase and contraction

In order to analyze the functional role of p62 and the $PKC\zeta$ -p62- $K_V1.5$ interaction, we analyzed the effects of U46619 (100 nM) on K_V currents in $p62^{-/-}$ and the corresponding wild-type mice. The magnitude of the currents, the threshold voltage for activation, the current-voltage relationship and the current inactivation (Fig. 3C and 3D) were similar in PASMC from wild-type and $p62^{-/-}$ mice (e.g. current density at +40 mV was 10.9 ± 1.3 and 11.6 ± 1.7 pA pF^{-1} , respectively, and at 200 ms current decayed by 12.7 ± 2.8 and $14.3 \pm 2.9\%$, respectively). As expected, U46619 caused a significant inhibition in the whole range of channel activation and depolarized the membrane in PASMC from wild-type mice (Fig. 3A, C and E). Current inactivation at +40 mV was also increased by U46619 (i.e. at 200 ms the current decayed by $21.7 \pm 2.9\%$, $p < 0.05$). However, the TXA_2 analogue had no effect on K_V currents in PASMC from $p62^{-/-}$ mice (Fig. 3B, D and E).

MOL #37002

Basal levels of $[Ca^{2+}]_i$ in $p62^{-/-}$ (184 ± 35 nM, $n=5$) were not significantly different from those in wild-type mice (170 ± 45 nM, $n=6$). We found that genetic inactivation of p62 abolished the increase in $[Ca^{2+}]_i$ induced by U46619 (Fig. 4B and 4C). However, the contractile response induced by the two concentrations of U46619 tested was remarkably similar in $p62^{-/-}$ and wild-type mice (Fig. 4D).

Role of $K_V1.5$ channels in TXA_2 -induced effects

$K_V1.5$ channels have been reported to be major contributors of K_V currents in PASMCs in several animal species. Fig. 5A shows $hK_V1.5$ current traces recorded in Ltk^- cells stably expressing $hK_V1.5$ channels. U46619 (100 nM) significantly inhibited $hK_V1.5$ currents. This inhibitory effect was only observed at the end of the depolarizing pulse; e.g. currents were almost unaffected at the peak ($4.6 \pm 2.4\%$ decrease, not significant) but reduced by $17.8 \pm 4.2\%$ after 200 ms ($n=4$, $p < 0.05$). In rat PASMCs, U46619 also inhibited K_V currents (Fig. 5B) as previously described (Cogolludo et al., 2003). The $K_V1.5$ channel blocker DPO-1 (Lagrutta et al., 2006) inhibited K_V currents in rat PASMCs. In the presence of DPO-1, U46619 produced no further inhibitory effects (Fig 5B). Therefore, we analyzed a possible interaction between $PKC\zeta$, $K_V1.5$ channels and p62. Rat pulmonary arteries were incubated for 30 s in the absence (control) or presence of U46619. Homogenates were immunoprecipitated with anti- $PKC\zeta$ or anti- $K_V1.5$ antibodies and the content of $K_V1.5$, $PKC\zeta$ or p62 in the immunoprecipitates was analyzed via Western blot. Fig. 5C shows that in immunoprecipitates of $K_V1.5$ both $PKC\zeta$ and p62 were present. The $K_V1.5$ - $PKC\zeta$ and the $K_V1.5$ -p62 association were $135 \pm 13\%$ ($n= 8$, not significant, $p = 0.06$) and $163 \pm 31\%$ ($n= 7$, $p < 0.05$), respectively, in U46619-treated vs untreated arteries. The $K_V1.5$ - $PKC\zeta$ interaction

MOL #37002

was also observed in immunoprecipitates of PKC ζ immunoblotted with the anti-K_V1.5 antibody (not shown).

Interaction of PKC ζ with K_V channels: role of p62

In order to determine the potential role of the PKC ζ scaffold protein p62, the PKC ζ -K_V1.5 interaction was analyzed by co-immunoprecipitation in lungs from wild-type and p62^{-/-} mice. Genetic inactivation of p62 in mice did not modify the expression levels of either PKC ζ or K_V1.5 channels in PASMC (Fig. 6A). In immunoprecipitates of PKC ζ from wild-type mice immunoblotted with the anti-K_V1.5 antibody a band of approx. 80 kDa was observed which presumably reflects the mature (glycosylated) form of the channel expressed in the membrane (Li et al., 2000). However, p62-deficient mice showed a weak PKC ζ -K_V1.5 co-immunoprecipitation (Fig. 6B).

DISCUSSION

By using non selective PKC inhibitors and the PKC ζ selective inhibitor (PKC ζ -PI) we suggested that PKC ζ was involved in the K_V channel inhibition and the contractile response induced by TXA₂ in rat pulmonary artery myocytes (Cogolludo et al., 2003; 2005). Herein, we confirmed the role of PKC ζ in native K_V currents by using PASMCs from PKC ζ ^{-/-} mice. Consistent with the essential role of K_V1.5 channels in the pulmonary vasculature, we show that the K_V1.5 inhibitor DPO-1 inhibited K_V currents in native rat PASMCs by approx. 50%

MOL #37002

and that the TXA₂ analogue U46619 had no further inhibitory effects. In addition, cloned human K_V1.5 channels expressed in Ltk⁻ cells were also inhibited by U46619. Moreover, our results demonstrate the interaction between PKCζ and K_V1.5 in both rat PA and mice lungs which was minimal in p62^{-/-} mice. Deletion of p62 abolished K_V channel inhibition and Ca²⁺ responses induced by TXA₂, further supporting the role of p62 as a key mediator between PKCζ and K_V1.5. However, our study also showed that the contractile response induced by U46619 in PA was similar in wild-type and p62^{-/-} mice.

In both rat and newborn porcine PASMC, U46619 inhibited K_V currents, depolarized cell membrane, increased [Ca²⁺]_i through Ca_L channels and induced a contractile response (Cogolludo et al., 2003; 2005). U46619 had no direct effect on Ca_L channels in voltage-clamped cells indicating that increased Ca²⁺ entry through Ca_L channels is secondary to membrane depolarization. Herein, we demonstrated that, in mice, U46619 also inhibits K_V currents in PASMC and induces a [Ca²⁺]_i response and vasoconstriction in isolated PA. The degree of K_V channel inhibition in mice PASMC (~25% at 100 nM U46619) was similar to that observed in porcine and in rat PA and was accompanied by a significant membrane depolarization. In rat and porcine PA, all these effects were inhibited by calphostin C and PKCζ-PI (Cogolludo et al., 2003; 2005). These experiments suggested a role for PKCζ as a link between TP receptors and K_V channels which was confirmed in the present study using PKCζ^{-/-} mice. The magnitude and current-voltage relationship of K_V currents were similar in the wild-type and knockout animals suggesting no changes in the channel proteins underlying K_V currents. Thus, genetic inactivation or pharmacological inhibition of PKCζ abolished the effects of U46619 on K_V currents or membrane potential in PASMC. In contrast, both approaches only partially inhibited (~50-70%) the Ca²⁺ signal induced by U46619 in rat and

MOL #37002

mice PA, indicating that, in addition to the PKC ζ -K $_V$ -Ca $_L$ pathway mechanisms increasing [Ca $^{2+}$] $_i$ (e.g. Ca $^{2+}$ release from intracellular stores) are also activated in response to U46619 (Snetkov et al., 2006).

The present experiments also indicate that in mice, PKC ζ contributes to the vasoconstriction induced by TP receptor activation. These results are in agreement with those obtained in rats and newborn piglets using PKC ζ -PI (Cogolludo et al., 2003; 2005). However, in two week old piglets (Cogolludo et al., 2005), PKC ζ -PI and the Ca $^{2+}$ channel blocker nifedipine almost fully inhibited U46619-induced increases in [Ca $^{2+}$] $_i$ but had no effect on U46619-induced contractile responses, i.e. there was a contractile response in the absence of changes in [Ca $^{2+}$] $_i$. Therefore, in these animals, the up-regulation of Ca $^{2+}$ -independent mechanisms for contraction (Somlyo and Somlyo, 2000) makes PKC ζ and the [Ca $^{2+}$] $_i$ signal redundant.

K $_V$ currents recorded in native PASMCs reflect the contribution of multiple K $_V$ channel proteins (e.g. in human PA, 22 transcripts of K $_V\alpha$ subunits: K $_V$ 1.1 to K $_V$ 1.7, K $_V$ 1.10, K $_V$ 2.1, K $_V$ 3.1, K $_V$ 3.3, K $_V$ 3.4, K $_V$ 4.1, K $_V$ 4.2, K $_V$ 5.1, K $_V$ 6.1 to -6.3, K $_V$ 9.1, K $_V$ 9.3, K $_V$ 10.1, and K $_V$ 11.1, and 3 of K $_V\beta$ subunits: K $_V\beta$ 1 to -3 have been identified by RT-PCR). However, K $_V$ 1.5 subunits are believed to be major contributors of the native K $_V$ currents in PA from different species and their activity is regulated by vasoactive factors such as 5-HT (Cogolludo et al., 2006) and hypoxia (Platoshyn et al., 2006). Therefore, we analyzed the effects of U46619 on the K $_V$ current carried by human cloned K $_V$ 1.5 channels expressed in mouse fibroblast (Ltk $^-$) cells. This cell line expresses endogenously the K $_V\beta$ 2.1 subunit which assembles with the transfected hK $_V$ 1.5 protein (Uelele et al., 1996). U46619 induced a weak but significant inhibitory effect on this current, suggesting that K $_V$ 1.5 channels are involved

MOL #37002

in the effects of TP receptor activation in native PASMCS. The small inhibition in this cell type probably reflects a lower efficacy of the signalling pathway compared to rat or mice PASMCS. Furthermore, after pharmacological inhibition of $K_V1.5$ channels with DPO-1, U46619 had no further inhibitory effects on K_V currents in rat PASMCS.

In the present paper we show that PKC ζ co-immunoprecipitates with $K_V1.5$ channels. In a previous study (Cogolludo et al 2003), we reported that U46619 induced the translocation of PKC ζ from the cytosolic to the membrane fraction. Therefore, TP receptor-induced K_V channel inhibition is associated with the translocation of PKC ζ to the plasma membrane where it interacts with $K_V1.5$ channels. This PKC ζ - $K_V1.5$ interaction is not necessarily a direct protein-protein interaction; it seems more likely that it is mediated by adaptor proteins. In this regard, it has been described that PKC ζ can interact with the β subunit $K_V\beta2$ of the K_V channel via the p62 adaptor protein (Gong et al., 1999). In immunoprecipitation experiments, we found that p62 was present in the $K_V1.5$ -PKC ζ complex. Even when the complex was constitutive, the association of p62 with $K_V1.5$ increased significantly by U46619. Furthermore, the PKC ζ - $K_V1.5$ co-immunoprecipitation was strongly reduced in p62^{-/-} mice lung indicating that p62 physically associates PKC ζ into the K_V channel complex.

$K_V\beta$ subunits function as molecular chaperones, and can directly regulate channel inactivation, voltage-dependence and current amplitude (Martens et al., 1999). p62 overexpression stimulates PKC ζ -dependent phosphorylation of $K_V\beta2$ (Gong et al., 1999) and induces a hyperpolarizing shift of K_V current activation in pheochromocytoma cells (Kim et al., 2004). Thus, we analyzed the effect of genetic inactivation of p62 on K_V currents and its

MOL #37002

modulation by TP receptor activation. K_V currents in PASMCs from $p62^{-/-}$ were similar to wild-type. As expected, U46619 had no effect on K_V currents in $p62^{-/-}$ PASMCs indicating that the $p62$ -dependent $PKC\zeta$ - $K_V1.5$ interaction is required for the inhibitory effect of TP receptor activation on K_V current.

Thus, genetic inactivation of $p62$ had a similar effect to genetic or pharmacologic inactivation of $PKC\zeta$ regarding K_V current modulation. Unexpectedly, we found that $p62$ gen deletion fully inhibited the Ca^{2+} response induced by U46619 in isolated PA as compared to a 50-70% inhibition by $PKC\zeta$ inactivation. More intriguingly, the contractile response to U46619 was not affected in PA from $p62^{-/-}$ mice. This contractile response in the absence of changes in $[Ca^{2+}]_i$ must then be attributed to Ca^{2+} -independent mechanisms (i.e. Ca^{2+} sensitization, Somlyo and Somlyo, 2000). This response to U46619 in $p62^{-/-}$ mice PA is similar to that observed in two week old piglet PA after inhibition of $PKC\zeta$, i.e. contraction without $[Ca^{2+}]_i$ signal (Cogolludo et al., 2005). In these animals, there is an up-regulation of Rho kinase (Bailly et al., 2004), a key enzyme in Ca^{2+} sensitizing mechanisms. In addition, Rho kinase inhibitors were more effective inhibiting U46619-contractions in these piglets than in newborn piglets or adult rats (Cogolludo et al., 2005). Thus, we speculate that the chronic downregulation of the $PKC\zeta$ - $p62$ - K_V - Ca_L dependent pathway, either at the level of K_V channel activity (as occurs in older piglets) or $p62$ ($p62^{-/-}$ mice), but not $PKC\zeta$ ($PKC\zeta^{-/-}$ mice) is compensated by upregulation of Ca^{2+} sensitization mechanisms.

In conclusion, $PKC\zeta$ modulates K_V channel function and is involved in pulmonary vasoconstriction induced by TP receptor activation. The interaction between $PKC\zeta$ and $K_V1.5$ and the inhibitory effect of U46619 in cloned human $K_V1.5$ channels suggest that these

MOL #37002

specific channel subtypes are functional targets for PKC ζ . The adaptor protein p62 is required for the PKC ζ -K $_V$ 1.5 interaction and hence for the inhibition of K $_V$ currents following TP receptor activation.

References

Archer S, Souil E, Dinh-Xuan AT, Schremmer B, Mercier JC, El Yaagoubi A, Nguyen-Huu L, Reeve HL, Hampl V (1998) Molecular identification of the role of voltage-gated K⁺ channels, Kv1.5 and Kv1.2, in hypoxic pulmonary vasoconstriction and control of resting membrane potential in rat pulmonary artery myocytes. *J Clin Invest* **101**:2319-2330.

Bailly K, Ridley AJ, Hall SM, Haworth SG (2004) RhoA activation by hypoxia in pulmonary arterial smooth muscle cells is age and site specific. *Circ Res* **94**:1383-1391.

Barnes PJ, Liu SF (1995) Regulation of pulmonary vascular tone. *Pharmacol Rev* **47**:87-131.
Cogolludo A, Moreno L, Lodi F, Frazziano G, Cobeno L, Tamargo J, Perez-Vizcaino F (2006) Serotonin inhibits voltage-gated K⁺ currents in pulmonary artery smooth muscle cells: role of 5-HT_{2A} receptors, caveolin-1, and K_v1.5 channel internalization. *Circ Res* **98**:931-938.

Cogolludo A, Moreno L, Lodi F, Tamargo J, Perez-Vizcaino F (2005) Postnatal maturational shift from PKC ζ and voltage-gated K⁺ channels to RhoA/Rho kinase in pulmonary vasoconstriction. *Cardiovasc Res* **66**:84-93.

Cogolludo A, Moreno L, Bosca L, Tamargo J, Perez-Vizcaino F (2003) Thromboxane A₂-induced inhibition of voltage-gated K⁺ channels and pulmonary vasoconstriction: role of protein kinase C ζ . *Circ Res* **93**:656-663.

MOL #37002

Duran A, Serrano M, Leitges M, Flores JM, Picard S, Brown JP, Moscat J, Diaz-Meco MT (2004) The atypical PKC-interacting protein p62 is an important mediator of RANK-activated osteoclastogenesis. *Dev Cell* **6**:303-309.

Frey RS, Gao X, Javaid K, Siddiqui SS, Rahman A, Malik AB (2006) Phosphatidylinositol 3-kinase gamma signaling through protein kinase Czeta induces NADPH oxidase-mediated oxidant generation and NF-kappaB activation in endothelial cells. *J Biol Chem* **281**:16128-16138.

Gayral S, Deleris P, Laulagnier K, Laffargue M, Salles JP, Perret B, Record M, Breton-Douillon M (2006) Selective activation of nuclear phospholipase D-1 by G protein-coupled receptor agonists in vascular smooth muscle cells. *Circ Res* **99**:132-139.

Godeny MD, Sayeski PP (2006) ANG II-induced cell proliferation is dually mediated by c-Src/Yes/Fyn-regulated ERK1/2 activation in the cytoplasm and PKCzeta-controlled ERK1/2 activity within the nucleus. *Am J Physiol Cell Physiol* **291**:C1297-307.

Gong J, Xu J, Bezanilla M, van Huizen R, Derin R, Li M (1999) Differential stimulation of PKC phosphorylation of potassium channels by ZIP1 and ZIP2. *Science* **285**:1565-9.

Halushka PV, Mais DE, Mayeux PR, Morinelli TA (1989) Thromboxane, prostaglandin and leukotriene receptors. *Annu Rev Pharmacol Toxicol* **29**: 213-239.

MOL #37002

Hirai T, Chida K (2003) Protein kinase C ζ (PKC ζ): activation and cellular functions, *J Biochem (Tokyo)* **133**:1-7.

Kim Y, Uhm DY, Shin J, Chung S (2004) Modulation of delayed rectifier potassium channel by protein kinase C zeta-containing signaling complex in pheochromocytoma cells. *Neuroscience* **125**:359-368.

Kim Y, Park MK, Uhm DY, Shin J, Chung S (2005) Modulation of delayed rectifier potassium channels by alpha1-adrenergic activation via protein kinase C zeta and p62 in PC12 cells. *Neurosci Lett* **387**:43-48.

Krotova K, Hu H, Xia SL, Belayev L, Patel JM, Block ER, Zharikov S (2006) Peptides modified by myristoylation activate eNOS in endothelial cells through Akt phosphorylation. *Br J Pharmacol* **148**:732-740.

Lagrutta A, Wang J, Fermini B, Salata JJ (2006) Novel, potent inhibitors of human Kv1.5 K⁺ channels and ultrarapidly activating delayed rectifier potassium current. *J Pharmacol Exp Ther* **317**:1054-1063.

Leitges M, Sanz L, Martin P, Duran A, Braun U, Garcia JF, Camacho F, Diaz-Meco MT, Rennert PD, Moscat J (2001) Targeted disruption of the zetaPKC gene results in the impairment of the NF-kappaB pathway. *Mol Cell* **8**:771-780.

MOL #37002

Li D, Takimoto K, Levitan ES (2000) Surface expression of Kv1 channels is governed by a C-terminal motif. *J Biol Chem* **275**: 11597-11602.

Liu LZ, Zhao HL, Zuo J, Ho SK, Chan JC, Meng Y, Fang FD, Tong PC (2006) Protein kinase Czeta mediates insulin-induced glucose transport through actin remodelling in L6 muscle cells. *Mol Biol Cell* **17**:2322-2330.

Martens JR, Kwak Y-G, Tamkun MM (1999) Modulation of Kv channel α/β subunit interactions. *Trends Cardiovasc Med* **9**:253-258.

Moscat J, Diaz-Meco MT (2000) The atypical protein kinase Cs. Functional specificity mediated by specific protein adapters. *EMBO Rep* **1**:399-403.

Perez-Vizcaino F, Cogolludo A, Tamargo J (1999) Modulation of arterial $\text{Na}^+\text{-K}^+\text{-ATPase}$ -induced $[\text{Ca}^{2+}]_i$ reduction and relaxation by norepinephrine, ET-1, and PMA. *Am J Physiol* **276**:H651-H657.

Platoshyn O, Brevnova EE, Burg ED, Yu Y, Remillard CV, Yuan JX (2006) Acute hypoxia selectively inhibits KCNA5 channels in pulmonary artery smooth muscle cells. *Am J Physiol Cell Physiol* **290**:C907-916.

Pozeg ZI, Michelakis ED, McMurtry MS, Thebaud B, Wu XC, Dyck JR, Hashimoto K, Wang S, Moudgil R, Harry G, Sultanian R, Koshal A, Archer SL (2003) In vivo gene transfer

MOL #37002

of the O₂-sensitive potassium channel Kv1.5 reduces pulmonary hypertension and restores hypoxic pulmonary vasoconstriction in chronically hypoxic rats. *Circulation* **107**:2037-2044.

Remillard CV, Tigno DD, Platoshyn O, Burg ED, Brevnova EE, Conger D, Nicholson A, Rana BK, Channick RN, Rubin LJ, O'connor DT, Yuan JX (2007) Function of Kv1.5 Channels and Genetic Variations in KCNA5 in Patients with Idiopathic Pulmonary Arterial Hypertension. *Am J Physiol Cell Physiol* **292**: C1837-C1853.

Salamanca DA, Khalil RA (2005) Protein kinase C isoforms as specific targets for modulation of vascular smooth muscle function in hypertension. *Biochem Pharmacol* **70**:1537-1547.

Shimoda LA, Sylvester JT, Booth GM, Shimoda TH, Meeker S, Undem BJ, Sham JS (2001) Inhibition of voltage-gated K⁺ currents by endothelin-1 in human pulmonary arterial myocytes. *Am J Physiol Lung Cell Mol Physiol* **281**:L1115-L1122.

Shizukuda Y, Buttrick PM (2002) Protein kinase C-zeta modulates thromboxane A₂-mediated apoptosis in adult ventricular myocytes via Akt. *Am J Physiol Heart Circ Physiol* **282**:H320-H327.

Snetkov VA, Knock GA, Baxter L, Thomas GD, Ward JP, Aaronson PI (2006) Mechanisms of the prostaglandin F₂α-induced rise in [Ca²⁺]_i in rat intrapulmonary arteries. *J Physiol* **571**:147-163.

MOL #37002

Somlyo AP, Somlyo AV (2000) Signal transduction by G-proteins, Rho kinase and protein phosphatase to smooth muscle and non-muscle myosin II. *J Physiol* **522**:177-185.

Valenzuela C, Delpon E, Tamkun MM, Tamargo J, Snyders DJ (1995) Stereoselective block of a human cardiac potassium channel (Kv1.5) by bupivacaine enantiomers. *Biophys J* **69**:418-427.

Uebele VN, England SK, Chaudhary A, Tamkun MM, Snyders DJ (1996) Functional differences in Kv1.5 currents expressed in mammalian cell lines are due to the presence of endogenous Kv beta 2.1 subunits. *J Biol Chem* **271**:2406-2412.

Ward JP, Knock GA, Snetkov VA, Aaronson PI (2004) Protein kinases in vascular smooth muscle tone--role in the pulmonary vasculature and hypoxic pulmonary vasoconstriction. *Pharmacol Ther* **104**:207-231.

Weir EK, Reeve HL, Huang JM, Michelakis E, Nelson DP, Hampl V, Archer SL (1996) Anorexic agents aminorex, fenfluramine, and dexfenfluramine inhibit potassium current in rat pulmonary vascular smooth muscle and cause pulmonary vasoconstriction. *Circulation* **94**:2216-2220.

Yuan XJ, Wang J, Juhaszova M, Gaine SP, Rubin LJ (1998a) Attenuated K⁺ channel gene transcription in primary pulmonary hypertension. *Lancet* **351**:726-727.

MOL #37002

Yuan X-J, Wang J, Juhaszova M, Golovina VA, Rubin LJ (1998b) Molecular basis and function of voltage-gated K⁺ channels in pulmonary arterial smooth muscle. *Am J Physiol* **274**: L621–L635.

MOL #37002

Footnotes:

Supported by Grants from Ministerio de Educación y Ciencia (CICYT: SAF2005-03770, AGL2004-06685, SAF2005-04609; FPU: L.M. and G.F., FPI: L.C.) and Fundación Mutua Madrileña.

Reprint request to: Francisco Perez-Vizcaino. Department of Pharmacology, School of Medicine, Universidad Complutense. 28040 Madrid. Spain. Phone: 34-913941477; Fax: 34-913941470. Email: fperez@med.ucm.es

¹Both authors contributed equally.

MOL #37002

Figure 1. TP receptor activation leads to K_v current inhibition and depolarization in PASMCs from $PKC\zeta^{+/+}$ (A,C,E) but not from $PKC\zeta^{-/-}$ (B,D,F) mice. Panels A and B show current traces for 200 ms depolarization pulses from -60 mV to +40 mV (in 10 mV increments) from a holding potential of -60 mV before (control) and after application of the TXA_2 analogue U46619 (100 nM). Panels C and D show the current-voltage relationship measured at the end of the 200 ms pulse (means \pm SEM of 5 cells). Panels E and F show the effects of U46619 (100 nM) on membrane potential recorded under current clamp conditions. *, ** indicate $p < 0.05$ and $p < 0.01$, respectively, vs. control (paired Student's t test).

Figure 2. PA from $PKC\zeta^{-/-}$ mice show reduced $[Ca^{2+}]_i$ and contractile responses induced by TP receptor activation. Panels A and B show simultaneous recordings of $[Ca^{2+}]_i$ (upper trace) and force (lower trace) in PA from $PKC\zeta^{+/+}$ and $PKC\zeta^{-/-}$, respectively, stimulated by 30 and 300 nM U46619. The averaged values (means \pm SEM of 5-7 PA) of U46619-induced increase in $[Ca^{2+}]_i$ and force are shown in panels C and D, respectively. * indicates $p < 0.05$ vs. $PKC\zeta^{+/+}$ (unpaired Student's t test).

Figure 3. TP receptor activation leads to K_v current inhibition and depolarization in PASMCs from wild-type (A,C,E) but not from $p62^{-/-}$ (B,D,F) mice. Panels A and B show current traces for 200 ms depolarization pulses from -60 mV to +40 mV (in 10 mV increments) from a holding potential of -60 mV before (control) and after application of the TXA_2 analogue U46619 (100 nM). Panels C and D show the current-voltage relationship measured at the end of the 200 ms pulse (means \pm SEM of 5-6 cells). Panels E and F show

MOL #37002

the effects of U46619 on membrane potential recorded under current clamp conditions.* indicates $p < 0.05$ vs. control (paired Student's t test).

Figure 4. PA from $p62^{-/-}$ mice show no $[Ca^{2+}]_i$ responses but preserved contractions induced by TP receptor activation. Panels A and B show simultaneous recordings of $[Ca^{2+}]_i$ (upper trace) and force (lower trace) in PA from $p62^{+/+}$ and $p62^{-/-}$, respectively, stimulated by 30 and 300 nM U46619. The averaged values (means \pm SEM of 5 PA) of U46619-induced increase in $[Ca^{2+}]_i$ and force are shown in panels C and D, respectively. * indicates $p < 0.05$ vs. $p62^{+/+}$ (unpaired Student's t test).

Figure 5. Role of $K_V1.5$ channels: TP receptor activation inhibits $K_V1.5$ currents and increases co-immunoprecipitation of $K_V1.5$ with $PKC\zeta$. Panel A: Current traces recorded in Ltk⁻ cells stably transfected with human $K_V1.5$ before (control) and after U46619 (100 nM) and current-voltage relationship (means \pm SEM of 4 cells) measured at the end of the 200 ms pulse. Depolarizing steps from -60 to +60 mV were applied from a holding potential of -60 mV. * indicates $p < 0.05$ vs. control (paired Student's t test). Panel B: Current traces recorded in rat PASMCs cells before (control) and after the U46619 (100 nM) (upper panel) or before (control), after DPO-1 (300 nM) and after DPO-1 plus U46619 (lower panel). Current-voltage relationships are shown at the right (means \pm SEM of 3-4 cells). * indicates $p < 0.05$ vs. control (paired Student's t test). Panel C: Rat pulmonary arteries were incubated for 30 s in the absence (control) or presence of U46619 (100 nM), frozen and homogenated. Homogenates were immunoprecipitated with anti- $K_V1.5$ antibodies and immunoblotted with

MOL #37002

anti-PKC ζ or anti-p62. Results are representative of samples from 7-8 mice. Each pair of bands (control and U46619) is obtained from the same animal.

Figure 6. Similar expression of PKC ζ and K $_V$ 1.5 but reduced interaction between PKC ζ and K $_V$ 1.5 in p62 $^{-/-}$ vs p62 $^{+/+}$. Panel A: Representative western blots of lung homogenates using anti-K $_V$ 1.5 and anti-PKC ζ antibodies. Panel B: Lung homogenates were immunoprecipitated with anti-PKC ζ antibodies and immunoblotted with anti-K $_V$ 1.5, membranes were re-blotted with the anti-PKC ζ antibody as a loading control. The graph shows the densitometric analysis of the K $_V$ 1.5 protein relative to PKC ζ and expressed as a percent of values in wild-type mice. . ** indicates $p < 0.01$ vs. wild-type.

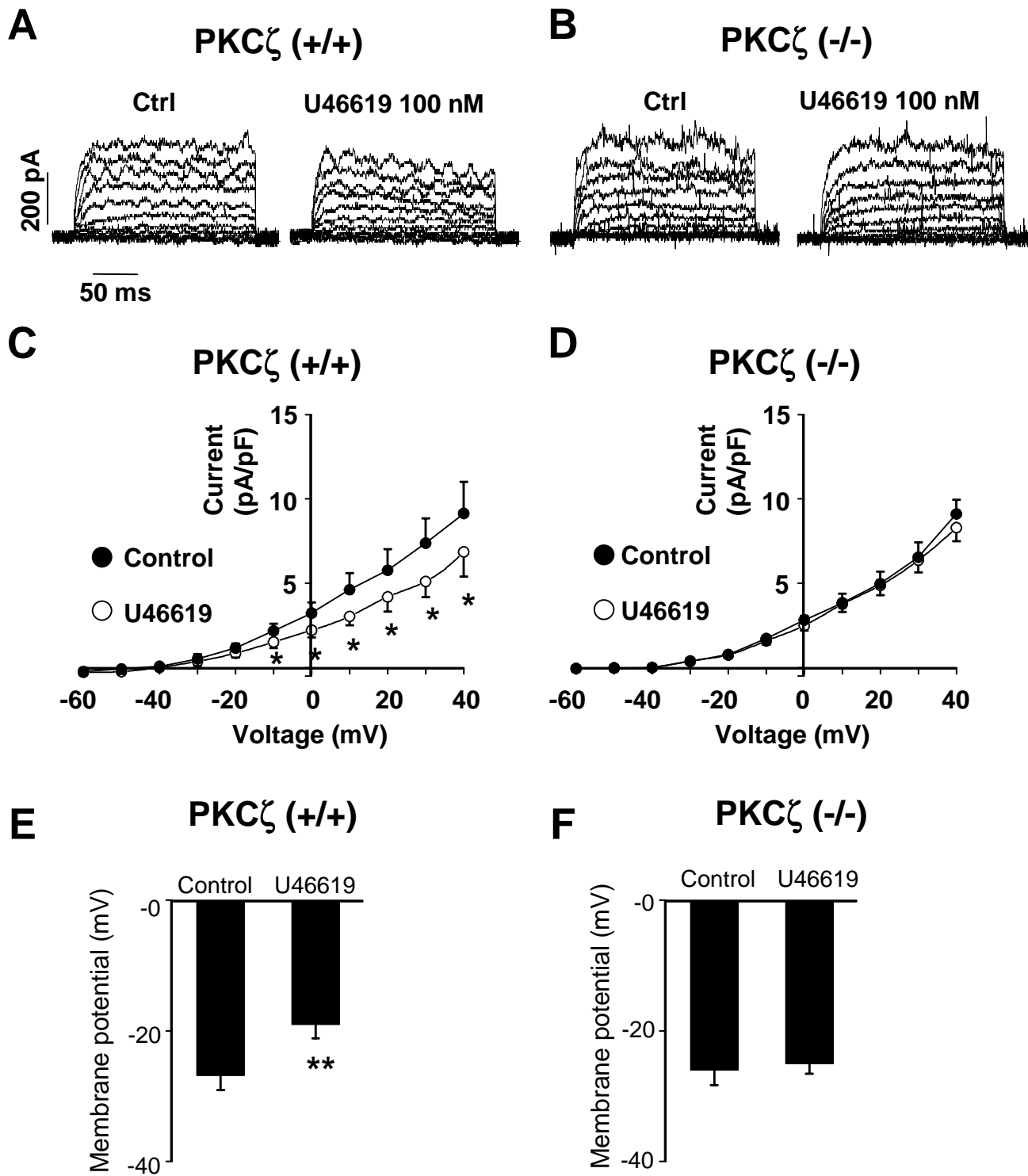


Figure 1

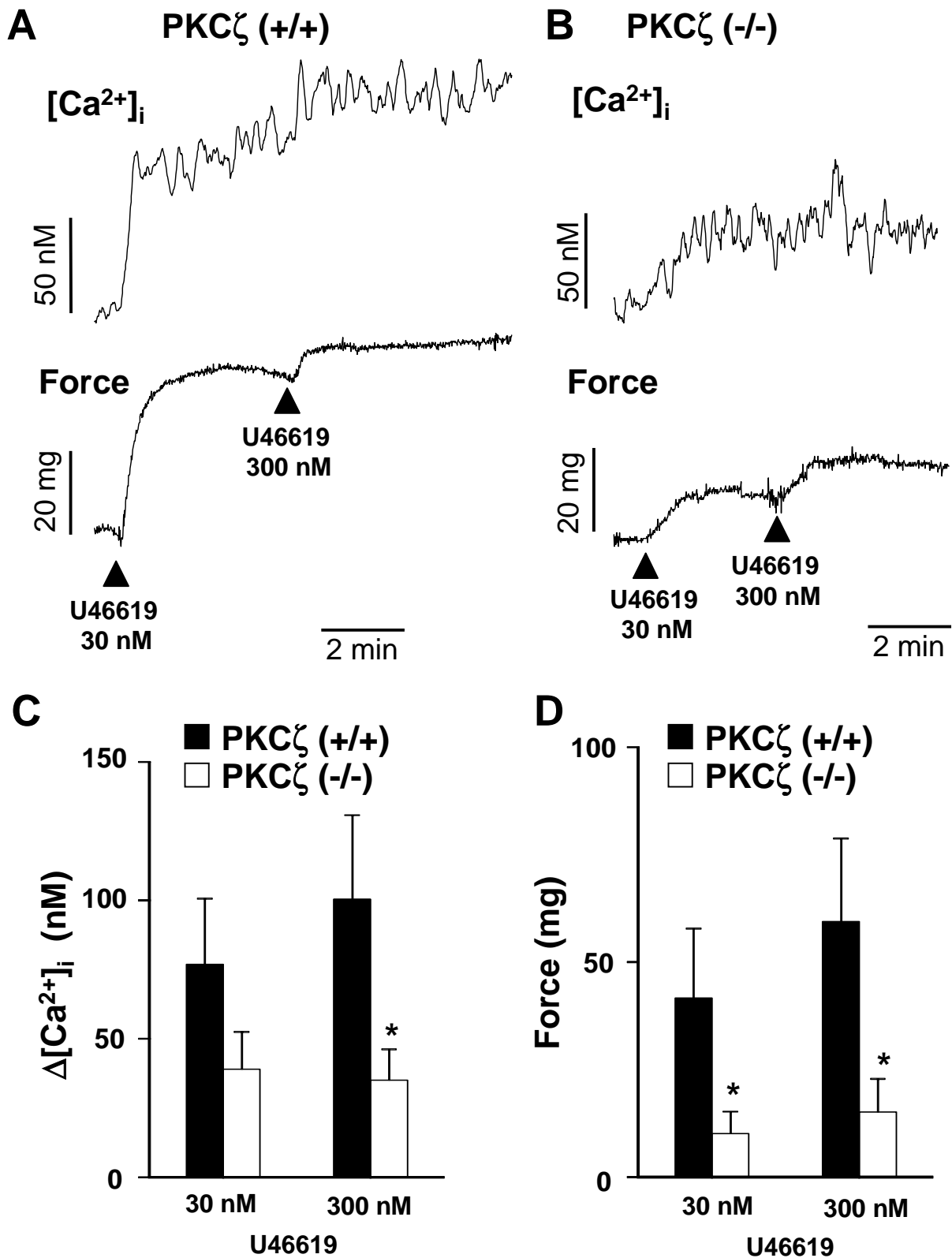


Figure 2

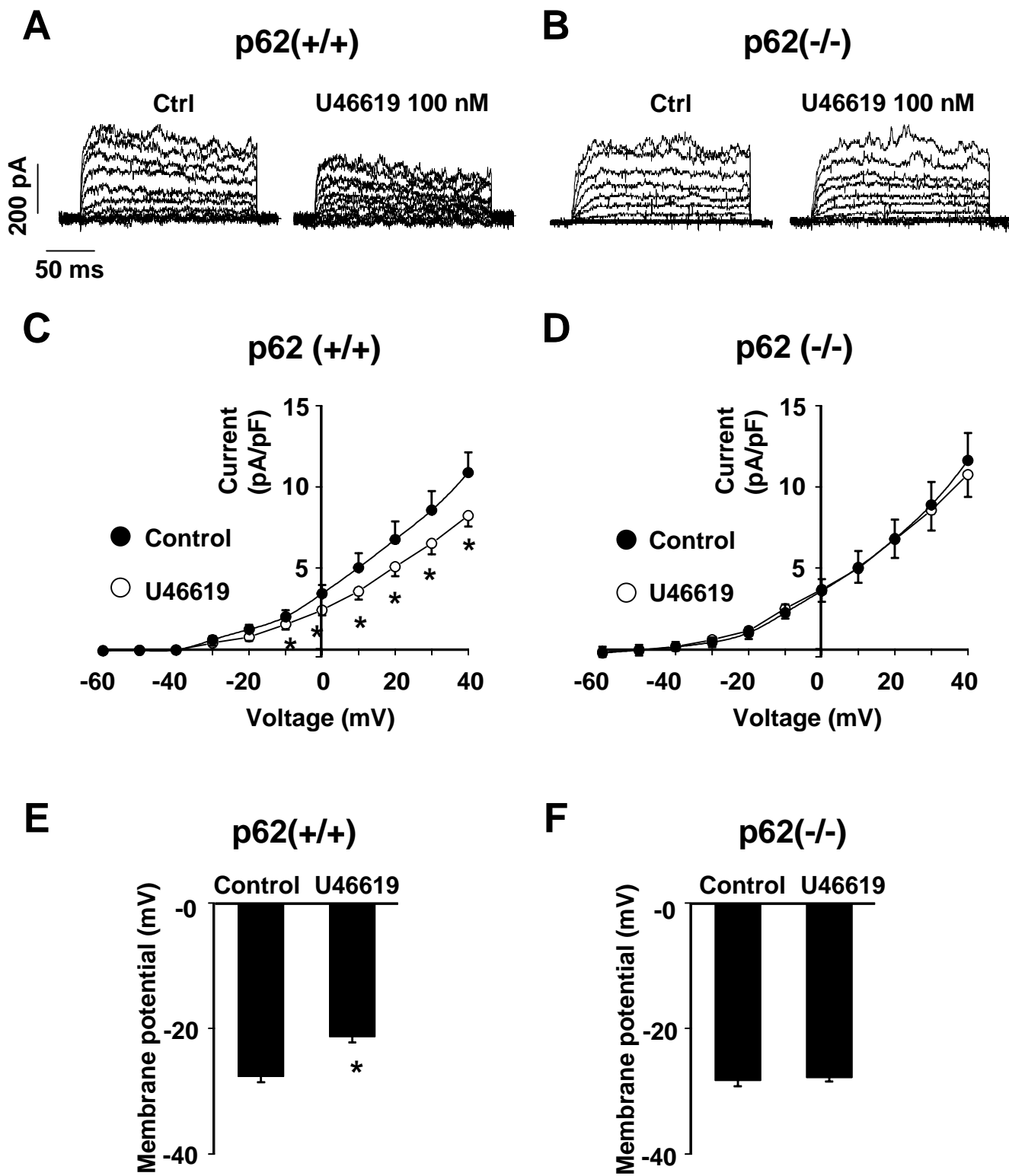


Figure 3

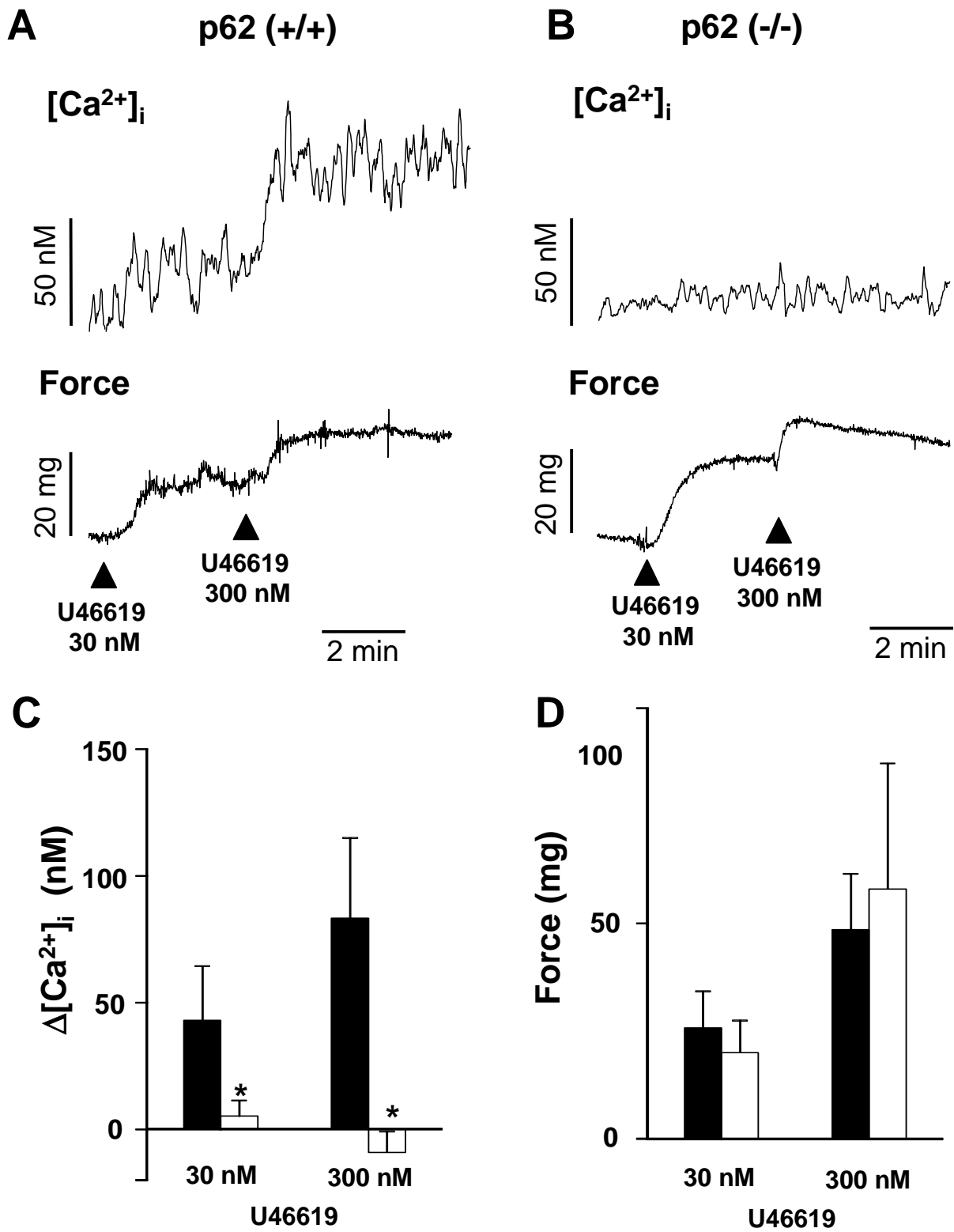


Figure 4

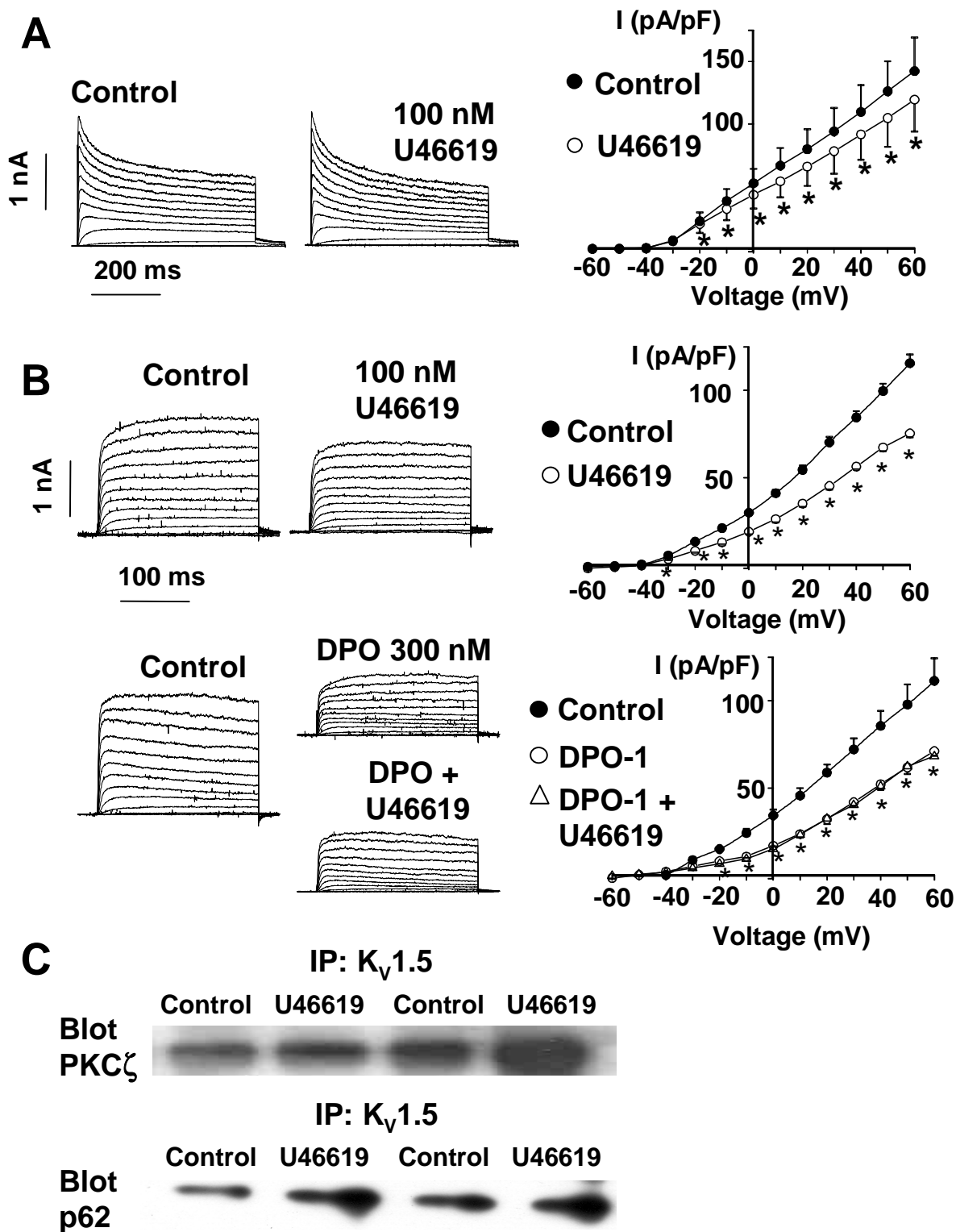


Figure 5

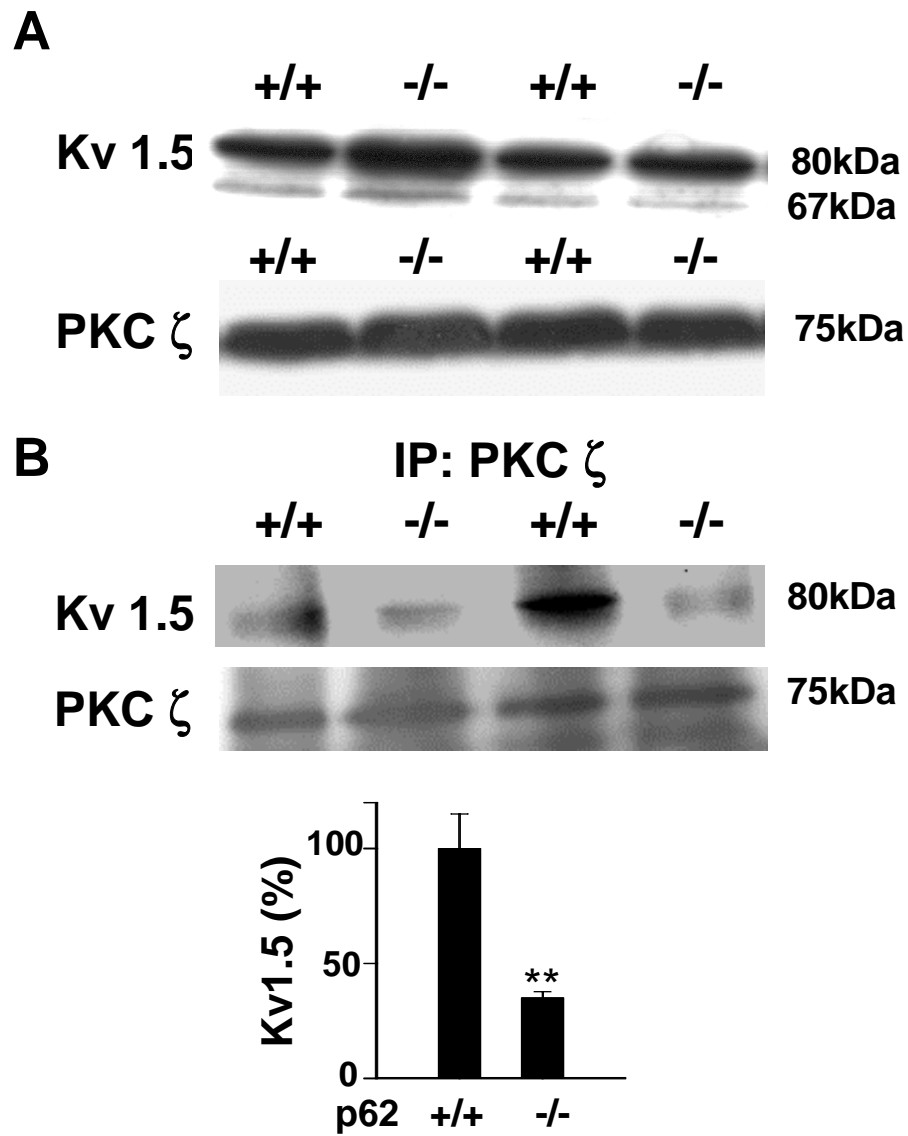


Figure 6